Talanta 210 (2020) 120675

Contents lists available at ScienceDirect

Talanta

journal homepage: www.elsevier.com/locate/talanta

# Simple and fast fabrication of microfluidic paper-based analytical device by contact stamping for multiple-point standard addition assay: Application to direct analysis of urinary creatinine

Arjnarong Mathaweesansurn[a,b], Suthathip Thongrod[a,b], Putthiporn Khongkaew[c], Chutima Matayatsuk Phechkrajang[a,d], Prapin Wilairat[a,e], Nathawut Choengchan[a,b,*]

[a] Flow Innovation-Research for Science and Technology Laboratories (FIRST Labs), Bangkok, 10520, Thailand
[b] Department of Chemistry and Applied Analytical Chemistry Research Unit, Faculty of Science, King Mongkut's Institute of Technology Ladkrabang, Chalongkrung Road, Ladkrabang, Bangkok, 10520, Thailand
[c] Faculty of Pharmaceutical Science, Burapha University, 169 Longhaad Bangsaen Road, Saensook, Muang, Chonburi, 20131, Thailand
[d] Department of Pharmaceutical Chemistry, Faculty of Pharmacy, Mahidol University, Rachathevi, Bangkok, 10400, Thailand
[e] National Doping Control Centre, Mahidol University, Bangkok, 10400, Thailand

ARTICLE INFO

*Keywords:*
Microfluidic paper-based analytical device
Multiple-point standard addition
Direct analysis
Creatinine
Image processing

ABSTRACT

In this work, a microfluidic paper-based analytical device (μPAD) for simultaneous multiple-point standard addition assay was fabricated by rubber stamping the hydrophobic barrier pattern onto a laboratory filter paper. The μPAD has a central zone from which an applied sample flows into eight surrounding narrow channels to which had been added the standard solutions. Each channel is connected to a circular area loaded with the reagent. The opposite end of this reagent zone is connected by second narrow channel to the final circular detection zone. The μPAD was applied to the measurement of creatinine in human urine. After addition of a urine sample, the orange-colored product arising from the Jaffé reaction is formed at the eight detection zones. A digital image of the μPAD is then recorded and the ratio of the red/green (R/G) intensity obtained using the ImageJ™ program is used in the quantitation of creatinine. The normal standard addition calibration line is constructed using the intensity ratio against the added creatinine concentrations (50–1000 mg $L^{-1}$). Good linearity was achieved ($r^2 > 0.99$). There were no significant differences between the creatinine content using an HPLC method (paired *t*-test at 95% confidence, $t_{stat} = 1.78$, $t_{critical} = 2.26$, n = 10). The use of simultaneous multiple-point standard addition calibration allows rapid determination of creatinine in urine with elimination of matrix interference.

## 1. Introduction

Creatinine (2-amino-1-methyl-*5H*-imidazole-4-one) is the metabolic waste product resulting from the non-enzymatic conversion of creatine and phosphocreatine in muscle. It is usually excreted from the body through glomerular filtration into urine at a relatively constant excretion rate [1]. The amount of excreted creatinine is proportional to an individual muscle mass [1,2]. Abnormal excretion levels indicate kidney malfunction. Thus, urinary creatinine concentration is an important biomarker for clinical diagnosis of kidney disease.

Various instrumental methods that allow analysis of creatinine in urine have been reported, including the traditional Jaffé method [3], enzymatic assays [4], capillary electrophoresis [5], high-performance liquid chromatography (HPLC) [6–8] and flow-based techniques [9–12]. The colorimetric Jaffé method is widely used because of its simplicity while the enzymatic methods are used for their high specificity. Separation techniques offer high accuracy and precision. Flow-based methods are very fast. Nevertheless, the instruments are expensive and bulky, so that these methods are not appropriate for "point-of-care" testing (POCT) [13].

In 2007, Whitesides et al. [14] created POCT devices, which they called "microfluidic paper-based analytical devices" or "μPADs". Since then, many analytical methods have employed paper, because of advantages, such as disposability, portability, cost-effectiveness and ease-of-use [15–19]. Paper-based devices for the determination of urinary creatinine have been reported based on enzymatic assay [20] and the Jaffé method [21–23]. These paper-based assays were calibrated using external calibration method. Boobphahom et al. designed a paper-based

* Corresponding author. Flow Innovation-Research for Science and Technology Laboratories (FIRST Labs), Bangkok, 10520, Thailand.
*E-mail address:* nchoengchan@gmail.com (N. Choengchan).

https://doi.org/10.1016/j.talanta.2019.120675
Received 29 September 2019; Received in revised form 21 December 2019; Accepted 23 December 2019
Available online 24 December 2019
0039-9140/ 

device with a modified composite electrode for the electrochemical quantitation of creatinine in serum [24]. Although these methods were successfully applied to real samples, pre-treatment protocols were required to eliminate matrix effects. Consequently, these assays were not applicable for direct determination.

Therefore, we aimed to develop a μPAD for direct analysis of urinary creatinine without requiring sample pre-treatment. We also designed a pattern of the hydrophobic barrier to perform simultaneous standard addition measurements on the paper platform to eliminate matrix effects. There have been few μPAD applications of standard addition assay. Martinez and co-workers [25] used a "single-point" standard addition on a paper-based device for glucose determination. The method may account for matrix effects; however, a single level spiked sample significantly affects accuracy [26,27]. Recently, Kappi et al. [28] presented calibrant-loaded paper-based devices for "multiple-point" standard addition assays. The devices contained multiple sensing areas, preloaded with reagents and known concentrations of standards. The sample was deposited separately in each one of the sensing zones. These devices were applied for the determination of various analytes but did not include creatinine. To the best of our knowledge, our work is the first report using the "multiple-point" standard addition method with a paper-based device for direct analysis of urinary creatinine. We selected the colorimetric Jaffé reaction for detection, owing to its simplicity. The hydrophobic barrier was fabricated by direct contact stamping [29–35] of an indelible ink onto the μPAD. The contact stamping method is simple, low-cost, and fast, providing one-step fabrication without sophisticated apparatus. Optimum conditions for the fabrication of the μPADs and for the detection of creatinine were investigated. We also compared the method with reversed-phase HPLC analysis.

## 2. Materials and methods

### 2.1. Chemicals and reagent preparation

All chemicals used were of analytical reagent grade and used as purchased. Deionized-distilled (DI) water (1.8 MΩ cm) was prepared using a Zeneer UP 900 water purification unit (Human Corporation, Seoul, Korea) and used throughout. A standard stock of 1 g $L^{-1}$ creatinine was prepared by dissolving an accurate weight of 0.1000 g anhydrous creatinine (Sigma-Aldrich, USA) in 100.0 mL of water. Working standard creatinine solutions were freshly prepared by appropriate dilution of the stock standard with DI water. A stock picric acid solution (0.052 mol $L^{-1}$) was prepared by dissolving ~2.9 g picric acid (Merck, USA) in 250 mL water. The alkaline picrate solution (0.025 mol $L^{-1}$ picric acid in 1.5 mol $L^{-1}$ NaOH) was prepared by mixing of 12.0 mL of stock picric acid and 12.5 mL of 3.0 mol $L^{-1}$ NaOH and diluted with DI water to obtain the final volume of 25.0 mL.

### 2.2. Fabrication of the μPAD

Fig. 1 illustrates the steps for fabrication of the μPAD by contact stamping. The custom-designed rubber stamp (Fig. 1A) and its plastic holder (total weight = 53 g) was manufactured by a local shop in Bangkok, Thailand, at a cost of 150 Baht (~5 USD). The stamp is covered with a lid before application of the ink, which is added by syringing 2.0 mL indelible ink (HORSE™ No. 2, Industry NAN MEE Co., Ltd., Thailand) into the ink filling hole (Fig. 1B). The ink is adsorbed by the rubber pad. Fig. 1C shows patterning of the hydrophobic barrier of the μPAD on a laboratory filter paper (Whatman™ No.1, 11 μm pore size, 180 μm thick) obtained by pressing the inked pad without any significant force for 5 s, to allow the ink to penetrate through the thickness of the filter paper. The embossed paper is dried at ambient temperature (~25 °C) for 5 min. The μPAD (Fig. 1D) is ready for use in the multiple-point standard addition assay of urinary creatinine.

### 2.3. Multiple-point standard addition assay for direct analysis of urinary creatinine

Fig. 2 shows the steps in the multiple-point standard addition assay for the direct analysis of urinary creatinine. We start by aliquoting 0.6 μL alkaline picrate solution on each circular reagent zone (Fig. 2A). The pad is dried using a hair dryer, set at minimum power, for 30 s. Next, transferring of 0.3 μL aliquot of the blank (water) to the channel a and a series of the standard creatinine solutions (50–1000 mg $L^{-1}$) to the inner channels marked b, c, d, e, f, g and h were carried out (Fig. 2B). The pad is blow-dried for 30 s. Then 55.0 μL urine sample is directly added to the central sample zone (Fig. 2C). The pad is then placed in a constant light illumination box. Exactly 5 min later (defined as the reaction time) a digital image of the μPAD is recorded using a tablet (Samsung Galaxy Tab S 8.4™) (Fig. 2D). The digital images are downloaded to a PC and processed using Image J™ software. A fixed area is set in the ImageJ™ software for measurement of the color images in the eight circular detection zones. The mean values of the Red (R), Blue (B) and Green (G) intensities within the defined area for each detection zone are recorded.

In this work, the visually observed orange color increased with increasing concentration of creatinine (see Fig. 2D). The mean value of R intensity was found to increase with increasing concentration of creatinine whereas the mean G intensity value decreased. But the mean B value remained almost constant. It was found that the ratio of the R/G intensity values increased proportionally with creatinine concentrations. Thus R/G intensity ratios are employed in constructing the multiple-point standard addition linear plot. In a separate study employing a μPAD (Fig. 1D), the alkaline picrate solution was added to the reagent zone, DI water was added to the inner channels and the sample zone. The image of the pad was recorded 5.0 min after addition of the water sample. It was found that the R/G intensity value was 1.0 ± 0.05 (n = 10 tests). Therefore, the value of the R/G intensity must always have values ≥ 1.0 for samples containing creatinine. The standard addition plot was constructed using value of (R/G - 1) *versus* the concentration of the standard creatinine. To obtain the creatinine concentration in the urine sample the following equation is employed: Conc. sample = (R/G −1) of un-spiked sample (zone a)/(slope of standard addition linear plot).

### 2.4. Validation

HPLC was used as a comparison method. The parameters of the HPLC system are: Symmetry™ C-18 column (3.9 mm × 150 mm, 5 μm) at 25 °C, isocratic elution with 20 mmol $L^{-1}$ ammonium dihydrogen orthophosphate (pH 7.4, Merck, USA) as mobile phase at flow rate of 0.8 mL $min^{-1}$, 20 μL injection volume and uv-absorbance detection at 210 nm. The chromatographic time was 7 min. Urine samples were diluted with the mobile phase at appropriate dilution ratios and filtered through a 0.22 μm nylon membrane prior to injection.

## 3. Results and discussion

### 3.1. Design of the μPAD for multiple-point standard addition assay

Fig. 1D shows the optimal μPAD design. It composes of (i) the single sample zone, (ii) the 8 reagent zones and (iii) the 8 detection zones. The sample zone is at the center of the device and is surrounded by eight lobes of reagent and detection zones. Each circular zone is connected to each other by a narrow channel. Each inner (reagent) zone is also connected to the central sample zone by a narrow channel. The blank (water) and a series of standard creatinine solutions are added to the inner channels. After sample addition into the central zone, the sample flows by capillary force, through the inner channels, the reagent zones, the outer channels and finally to the detection zones, where a colored product develops. With this design, the multiple-point standard

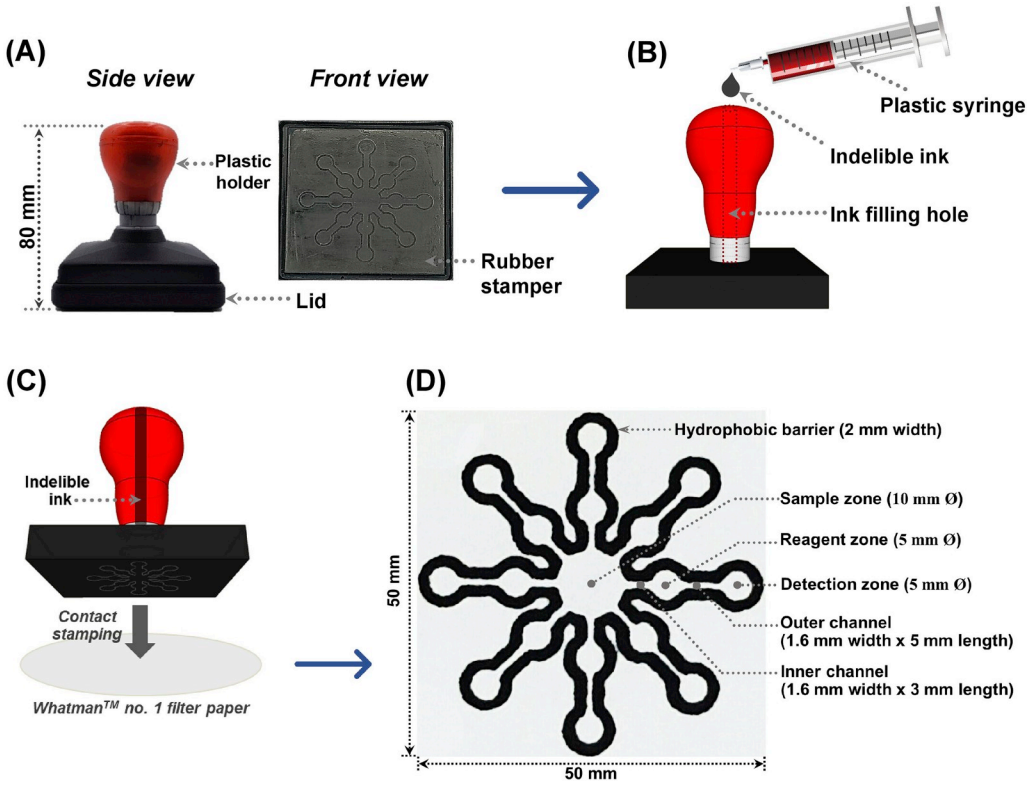


**Fig. 1.** Illustrations of the fabrication steps of the μPAD by contact stamping. **(A)** Photograph of the custom-designed stamping device, **(B)** ink filling, **(C)** stamping of pattern of the hydrophobic barrier on paper and **(D)** the final design of the μPAD for the multiple-point standard addition assay.

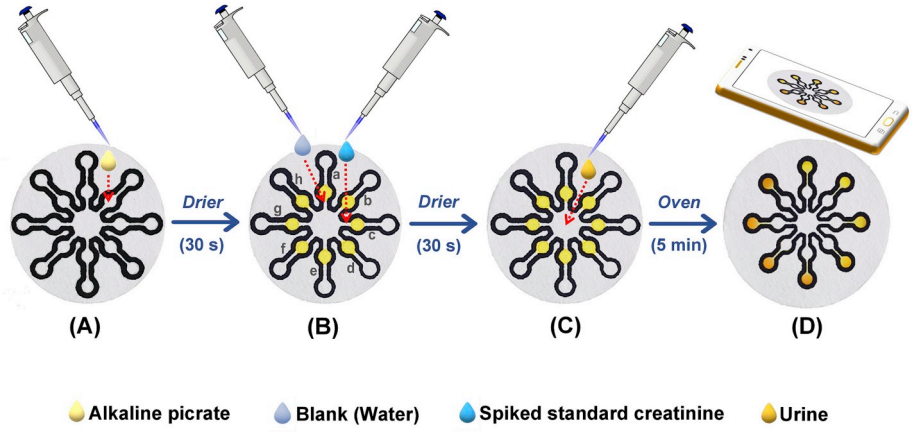


**Fig. 2.** Pictorial representation of the steps in the application of the picrate reagent, the water blank solution, the standard solutions of creatinine and the final recording of the image of the μPAD by a tablet camera.

addition measurements is simultaneously achieved [36–38]. The eight detection zones are recorded at the same time, so there is no effect from variation of the lighting condition.

It may be of interest that in the development of the design of the μPAD, only two zones, the sample and the detection zones, were employed. The reagent solution was added onto the detection zones and the standard solutions onto the channels connecting the detection zones with the central sample area. However, the colored product in the detection zones were non-uniform with "coffee ring" [39] patterns (see Fig. S1A). We tried to eliminate this problem by lengthening the channels. The color complex was still formed close to the hydrophobic barrier (Fig. S1B). This effect was resolved with the design of three separate zones (see Fig. 1D).

### 3.2. Selection of the ink and optimization of the dimensions of the hydrophobic barrier

#### 3.2.1. Choice of ink

Three commercially available indelible inks (Fig. 3) were tested by stamping onto Whatman™ No. 1 filter paper as a circular spot *ca.* 5 mm in diameter. All of ink were described as a "waterproof" ink by the manufacturers and were employed without any modification. The ink spot was dried at room temperature (5 min) for complete evaporation of the ink solvent. The hydrophobicity of the dry ink was characterized by placing a 3.0 μL water drop on its surface. Fig. 3A shows that all inks were hydrophobic; the water droplets had high contact angle with the ink surface and were not absorbed. However, penetration of the ink through the entire thickness of the paper to the underside was observed only with "Brand 1" (Fig. 3B). "Brand 1" ink was less viscous than

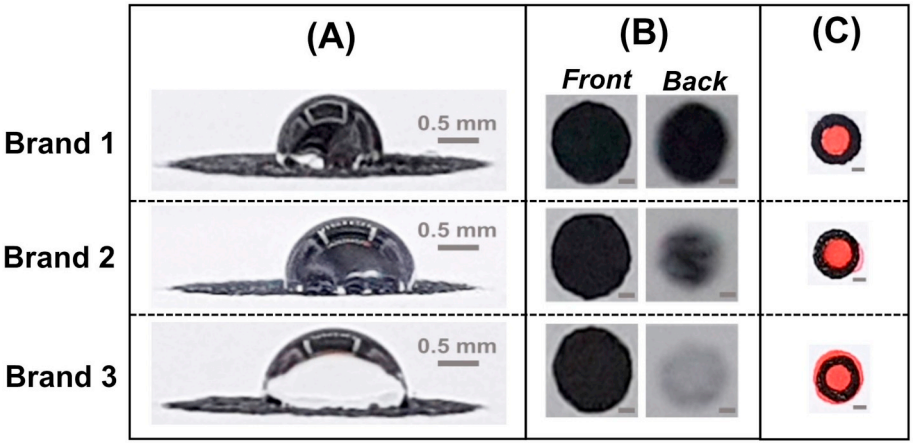


**Fig. 3. (A)** Images of a 2-μL water droplet on top of the ink spots, obtained by contact stamping of three brands of the commercially available indelible ink onto the surface of the paper. **(B)** Images of the ink spots on the front and reverse side of the paper. **(C)** Images of 2-μL aqueous red dye solution applied to a pad with circular hydrophobic barrier. Note: (i) Whatman™ filter paper No. 1 was used throughout all investigations. (ii) The scale lines in Fig. 3 (B) and **(C)** represent 2 mm length. (For interpretation of the references to color in this figure legend, the reader is referred to the Web version of this article.)

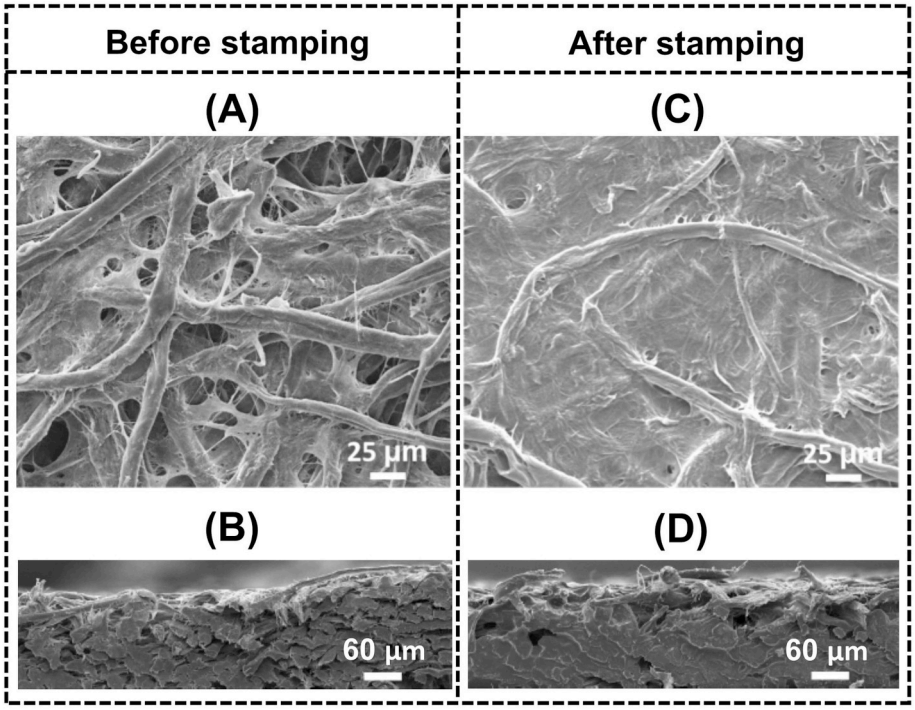


**Fig. 4.** SEM images showing the morphology of the paper before and after stamping of the selected indelible ink. **(A)** and **(C)** are the front view. **(B)** and **(D)** are the cross-sectional view.

"Brand 2" and "Brand 3". The SEM image in Fig. 4C shows that the porous structure of the paper substrate was entirely covered by the ink of "Brand 1". Fig. 4D also confirms that "Brand 1" ink penetrated and filled the cellulose pores of the paper. Since "Brand 2" and "Brand 3" inks were not absorbed throughout the thickness of paper, when a 1.0 μL aliquot of red dye solution was applied to a circular pattern ring the ink leaked out beneath the hydrophobic barrier, making the μPAD channel unusable (see Fig. 3C). "Brand 1" was therefore selected as the suitable ink. This selected ink was found to be resistant to both the alkaline reagent and creatinine solution (data not shown).

### 3.2.2. *Optimization of dimensions of the hydrophobic barrier*

Suitable dimensions of the width of the barrier, the length and width of the channel, as well as the diameter of the circular reagent and detection zones were investigated. The optimal barrier width was selected by applying the leakage test using a circular barrier pattern of 3 mm inner diameter. The width was varied from 0.4 to 1.6 mm, respectively. Results in Table 1 indicate that some sections of the barrier were missing for barrier width of 0.4 and 0.8 mm. This led to leakage of the red dye solution out of the application zone. At 1.2 and 1.6 mm, the circular barriers were intact, and no leakage was observed. A barrier of 1.2 mm width was chosen because, for this line width, the width of the printed line was not different from the width of the embossing rubber stamp.

The effect of the channel width was examined using the pattern shown in Fig. S2. The channel of various widths (1.0–2.4 mm) was connected to a circular area of paper of 6 mm diameter. When the channels were less than 1.4 mm wide the black ink spread and blocked the channel. For channels with width ≥1.6 mm, the flow of the red dye was too slow. Thus the 1.6 mm wide channel was selected.

The effect of the lengths of the two channels was evaluated using the pattern shown in Fig. 5 which has only one lobe connected to the sample area. Aliquots of 0.6 μL 0.025 mol $L^{-1}$ picric acid in 1.5 mol $L^{-1}$ NaOH and 55 μL standard creatinine (200 mg $L^{-1}$) were dropped onto the reagent (R) and the sample (S) zones. For the inner channel (connecting the sample area), the shortest length (3 mm) was selected because that led to the fastest analysis time. The outer channel is the reaction flow path and therefore the channel length would affect not

**Table 1**
Summary of the effect of the hydrophobic barrier width, fabricated by contact stamping of the selected indelible ink on the Whatman No. 1™ filter paper.

| Hydrophobic barrier width (mm) | | Leakage test[a] |
|---|---|---|
| Expected width[b] | Observed width [c] (Mean ± SD, n = 4) | |
| 0.4 | 0.9 ± 0.1 |  |
| 0.8 | 1.3 ± 0.2 |  |
| 1.2 | 1.2 ± 0.1 |  |
| 1.6 | 1.8 ± 0.2 |  |

Note.
[a] The leakage test was performed by dropping of 2.0 μL of red dye solution onto the patterning line (inner diameter = 3.0 mm). Each image is a representative among 4 replicate results.
[b] and [c] are the hydrophobic barrier width that are appeared on the rubber stamper and on the filter paper, respectively.

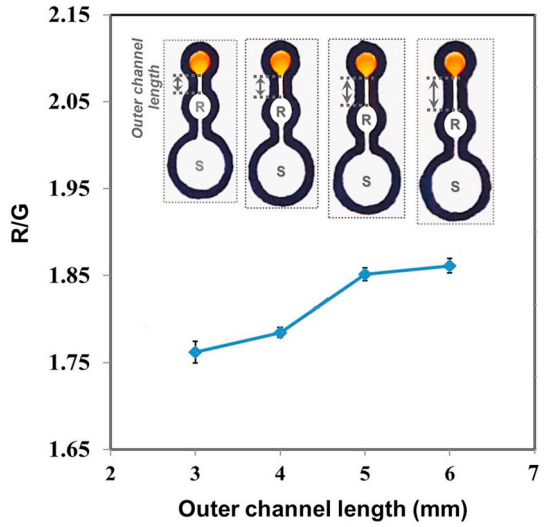


**Fig. 5.** Effect of the length of the outer channel of the μPAD on the R/G color intensity value at the detection zone. (For interpretation of the references to color in this figure legend, the reader is referred to the Web version of this article.)

only the time for the reactants to reach the detection zone, but also sensitivity of the analysis. The result sin Fig. 5 show that the R/G intensity ratio increased with channel length. As a compromise between sensitivity and analysis time, 5 mm channel length was chosen.

The selection of the diameters of the reagent and the detection zones are presented in Figs. S3A and B, respectively. A 0.6 μL volume of red dye solution was added to the reagent zone of various diameters. The 4 mm diameter was too small to accommodate the dye solution which spread out into the two channels. However, the 6 mm diameter was too large, and the dye did not fully fill the reagent area (see Fig. S3A). Thus the 5 mm diameter size of the reagent zone was chosen. The effect of the detection zone diameter was investigated by adding 0.6 μL aliquot of the picric acid reagent onto the reagent zone and 55 μL standard creatinine (200 mg $L^{-1}$) onto the sample zone. Results in Fig. S3B show that for the 4 mm diameter overflow of the colored product into the outer channels was observed. For the 6 mm diameter, a longer time was necessary for the liquid to spread completely over the detection zone. Thus the 5 mm diameter size for the detection zone was selected.

### 3.3. Optimization for detection of creatinine

#### 3.3.1. Sample and reagent volume

Effects of sample and reagent volumes are illustrated in Fig. S4. For selection of the optimal volume of sample, it was found that both 55 and 60 μL aliquots of the red dye solution when added to the central sample zone completely spread over all hydrophilic areas of the μPAD (Fig. S4A). However, 55 μL was chosen for lower sample consumption. For selection of the volume of reagent, addition of 0.5 μL of the red dye to the reagent zone was not sufficient to completely fill the reagent zone (Fig. S4B). Using larger volumes (0.7 and 0.8 μL), the red dye solution overflowed into the two connecting channels. Therefore, the optimal reagent volume was 0.6 μL.

#### 3.3.2. Concentrations of picric acid and NaOH

The effect of the picric acid concentration was examined by dropping 0.3 μL aliquot of various concentrations of standard solutions of creatinine (50–1000 mg $L^{-1}$) onto the μPAD in Fig. 1D. The concentration of picric acid was varied from 0.0125 to 0.1 mol $L^{-1}$, with the NaOH concentration fixed at 1.0 mol $L^{-1}$. Table 2 shows that the sensitivity of analysis increased with the picric concentration. As a compromise between reagent consumption and sensitivity, the concentration of 0.025 mol $L^{-1}$ picric acid was selected. The effect of NaOH concentration was studied by dropping 55 μL aliquot of 500 mg $L^{-1}$ creatinine onto the sample zone (S) and 0.6 μL 0.025 mol $L^{-1}$ picric acid in various NaOH concentrations (0.2–1.5 mol $L^{-1}$) onto the reagent (R) zones in Fig. 6. The R/G intensity ratio increased with the NaOH concentration. Concentration of NaOH of 2.0 mol $L^{-1}$ led to precipitation of picric acid due to its lower solubility in highly alkaline solution [23]. Thus, the concentration of 1.5 mol $L^{-1}$NaOH was selected as it gave the highest intensity.

#### 3.3.3. Reaction time

The reaction time is defined as the time interval between the addition of the standard/sample solution to the μPAD (see Fig. 2A) and the recording of the image (see Fig. 2D). Fig. S5 shows that when the reaction time was varied from 1.0 to 5.0 min, the intensity increased steeply but remained constant for longer reaction time (maximum time 30 min). Therefore, 5.0 min was chosen as the optimal reaction time.

Table S1 summarizes the optimization parameters discussed in the previous sections with the range of parameter values and the final selected value.

### 3.4. Analytical characteristics

Using the selected parameters in Table S1, good linearity ($r^{2>}$ 0.99) was obtained over a wide range of creatinine concentration (50–1000 mg $L^{-1}$). Reproducibility of production of the pads was verified by applying 50 mg $L^{-1}$ creatinine to ten different μPADs: a relative standard deviation (RSD) of 2.1% was obtained, demonstrating high precision. This value is smaller than the other studies [20–23] as shown in Table 3. The limit of determination (LOD) was 16.9 mg $L^{-1}$ (calculated using $2S_{y/x}$/slope of calibration [40]. This value is sufficient

**Table 2**
Effect of the concentration of picric acid on sensitivity of analysis of creatinine.

| Concentration of picric acid (mol $L^{-1}$) in 1.5 mol $L^{-1}$ NaOH | Recorded image of the μPAD | Calibration equation[a] | $r^2$ |
|---|---|---|---|
| 0.0125 | 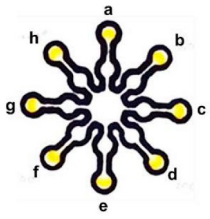 | y = (1.63 ± 0.03)×$10^{-4}$ x + (1.16 ± 0.01) | 0.989 |
| 0.025 | 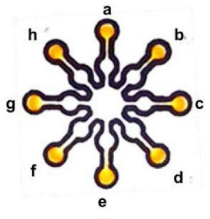 | y = (2.89 ± 0.04)×$10^{-4}$ x + (1.28 ± 0.02) | 0.995 |
| 0.05 | 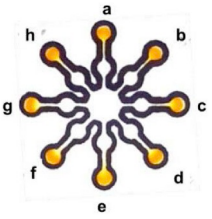 | y = (3.33 ± 0.02)×$10^{-4}$ x + (1.36 ± 0.02) | 0.992 |
| 0.1 | 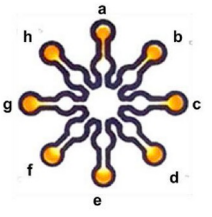 | y = (4.23 ± 0.01)×$10^{-4}$ x + (1.41 ± 0.04) | 0.992 |

The optical images of the studied μPADs are presented as the following optical images. Each image is a representative among 3 replicate results. a to h are 0, 50, 200, 300, 600, 800 and 1000 mg $L^{-1}$.

[a] x: standard creatinine concentration (0–1000 mg $L^{-1}$), y: value of R/G intensity.

for effectively measuring human urinary creatinine concentrations. The minimum value of creatinine in real human urine has been set 50 mg $L^{-1}$ [41].

The contact stamping method is simple. The handheld rubber stamp is lightweight (53 g) and low cost (~5 USD). Fabrication does not need sophisticated instruments. This allows fabrication in places where access to complex fabrication technology is limited.

This paper-based device was designed so that the multiple-point standard addition is carried out simultaneously. Standard addition method eliminates matrix effect of the urine sample. Sample preparation procedure, such as extraction, centrifugation and dilution, for elimination of the sample matrix effect is thus not required. For other paper-based devices for determination of creatinine [20–23], urine sample preparation prior to the analysis was necessary because external calibration was employed for quantification of the creatinine.

Even though, our method requires pre-spotting of multiple solutions, it is simpler and more practical than the traditional standard addition method, which is time-consuming since for each sample, several solutions must be prepared and measured separately.

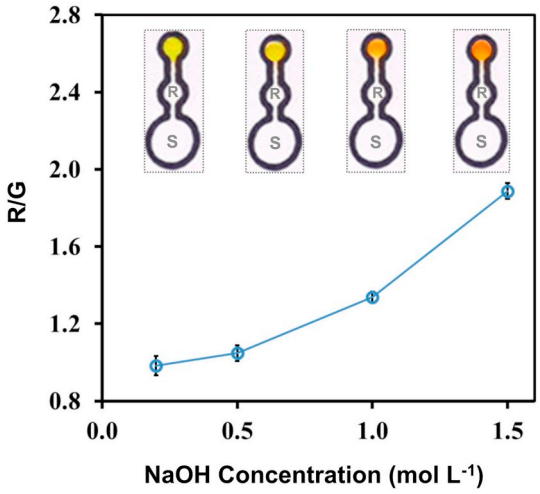


**Fig. 6.** Effect of NaOH concentration on the R/G color intensity value at the detection zone. S: Sample zone (10 mm diameter), R: reagent zone (5 mm diameter) and D: detection zone (5 mm diameter. (For interpretation of the references to color in this figure legend, the reader is referred to the Web version of this article.)

### 3.5. Application to urine samples: recovery and validation

To verify its practicability, the developed method was applied to analysis of creatinine in urine samples from healthy persons. Urine samples were directly measured without any pre-treatment. Recovery was measured by adding standard creatinine solution to urine samples to obtain the final added concentration of 500 mg $L^{-1}$. It is observed in Table 4 that the recoveries are in the range of 98.1–104% (mean recovery: (101.6 ( ± 2.1) %). Thus, the method is free from the sample matrix effect. Color of urine sample did not affect the accuracy of the results as shown by comparison with measurements using HPLC (see Table 5). This may be due to the small volume of the sample (55 μL) and adsorption of the color compounds by the paper itself.

Fig. 7 shows an optical image of the μPAD (Fig. 7A) and the corresponding standard addition linear graph (Fig. 7B) for quantitation of the creatinine content in a urine sample. The method was validated by comparison of results using the μPAD with the results from reversed-phase HPLC measurements (Table 5). There was no significant difference based on paired *t*-test [40] at 95% confidence ($t_{stat}$ = 2.01, $t_{critical}$ = 2.56, n = 10 samples).

## 4. Conclusion

A new patterning of μPAD was fabricated using a contact stamping method for simultaneous multiple-point standard addition assay of creatinine in human urine. The single step stamping, with a low-cost rubber stamp, was easy for patterning the hydrophobic barrier on the paper platform. The μPAD was successfully tested for quantitative analysis of the creatinine content. The standard addition plot was linear over a wide concentration range of creatinine (50–1000 mg $L^{-1}$) with $r^2 > 0.99$. The limit of quantitation (LOQ) was 16.9 mg $L^{-1}$, suitable for measuring human urinary creatinine concentrations. The developed method also provided high precision (2.1% RSD). The measurement was completed in 5 min. The urinary creatinine contents agreed well with HPLC measurements. This confirms that our method is accurate. Using standard addition method, direct analysis of urine was accomplished without requirement of the sample pre-treatment for elimination of the matrix effect. Therefore, the developed μPAD is capable for point-of-care measurements of human urinary creatinine.

**Table 3**
Comparison of the methodologies and the characteristics of the paper-based devices for determination of creatinine in human urine.

| Fabrication of the paper-based device | Detection principle | Sample pretreatment | Quantification method | Working range (mg $L^{-1}$) | LOD (mg $L^{-1}$) | RSD (%) | [Ref] |
|---|---|---|---|---|---|---|---|
| Cutting[a] | Enzymatic assay | Centrifugation (5 min) and dilution with buffer | External calibration | 25–250 | 20 | 11.6 | [20] |
| Coating[b] | Colorimetry | Dilution with 1.0 mol $L^{-1}$ and extraction on paper (12 min) | External calibration | 10–60 | 4.2 | < 10 | [21] |
| Wax printing[c] | Colorimetry | Centrifugation (5 min) and dilution with water | External calibration | 22.6–113 | 9 | 5.8 | [22] |
| Wax printing[c,d] | Colorimetry | Dilution and air bubbling | External calibration | 50–600 | 15.7 | < 5 | [23] |
| Contact stamping | Colorimetry | Without pretreatment (Direct analysis) | "Paper-based" Standard addition | 50-1000 | 16.9 | 2.1 | *This work* |

Note.
[a] Cutting of Whatman No. 3 filter paper and dipping one end of the paper into a melted wax for creation of the hydrophobic holder zone.
[b] Coating of Whatman No. 1 filter paper with 3-proppylsulfonic acid trimethoxysilane for extraction of creatinine on the paper platform.
[c] The masking pattern was printed onto the surface of Whatman No. 1 filter paper with the wax printer.
[d] The paper-based device was fabricated for simultaneous determination of creatinine and uric acid.

**Table 4**
Recovery of the developed paper-based device for the determination of creatinine in urine.

| Sample | Urinary creatinine concentration mg $L^{-1}$ (Mean ± SD, n = 3) | | | Recovery (%) |
|---|---|---|---|---|
| | Original | Spiked | Found | |
| S1 | 211.7 ± 1.9 | 500 | 713.7 ± 1.6 | 100 |
| S2 | 180.1 ± 1.7 | 500 | 698.5 ± 0.5 | 104 |
| S3 | 231.7 ± 0.9 | 500 | 735.6 ± 2.1 | 101 |
| S4 | 198.5 ± 0.4 | 500 | 712.7 ± 1.2 | 103 |
| S5 | 109.1 ± 2.7 | 500 | 599.9 ± 1.7 | 98.1 |
| S6 | 225.7 ± 1.7 | 500 | 738.9 ± 1.5 | 103 |
| S7 | 240.8 ± 2.5 | 500 | 753.2 ± 2.0 | 102 |
| S8 | 145.2 ± 1.1 | 500 | 638.7 ± 0.8 | 98.7 |
| S9 | 131.3 ± 2.5 | 500 | 640.5 ± 1.2 | 102 |
| S10 | 93.8 ± 1.2 | 500 | 611.9 ± 2.7 | 104 |

**Table 5**
Comparison of the urinary creatinine concentrations determined by this work and by the reversed-phase HPLC measurement.

| Sample | Urinary creatinine concentration (Mean ± SD, n = 3) | |
|---|---|---|
| | This work | HPLC |
| U1 | 132.70 ± 1.31 | 128.01 ± 0.02 |
| U2 | 144.49 ± 1.04 | 134.46 ± 0.31 |
| U3 | 179.63 ± 3.06 | 167.54 ± 0.04 |
| U4 | 180.60 ± 1.59 | 171.88 ± 1.73 |
| U5 | 180.00 ± 2.56 | 178.5 ± 0.01 |
| U6 | 240.83 ± 0.45 | 249.15 ± 1.89 |
| U7 | 339.70 ± 1.57 | 333.43 ± 0.88 |
| U8 | 336.40 ± 1.08 | 344.61 ± 3.26 |
| U9 | 370.87 ± 2.45 | 353.56 ± 0.30 |
| U10 | 589.90 ± 1.50 | 579.30 ± 1.08 |

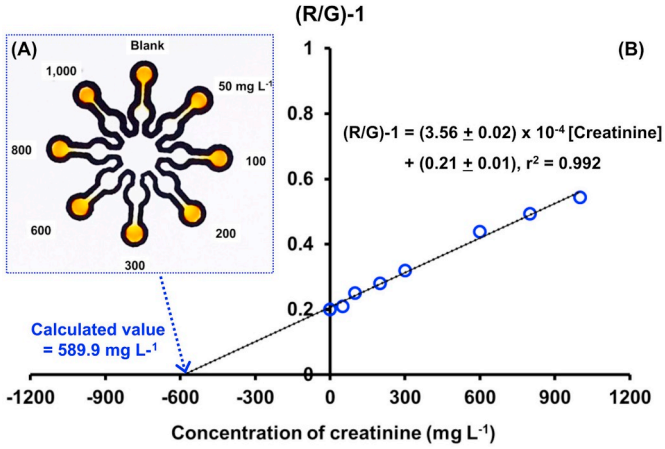


**Fig. 7.** An example of **(A)** the optical image of the μPAD and **(B)** its corresponding standard addition calibration for quantitation of the creatinine content in urine sample.

## Acknowledgements

Financial support from the Faculty of Science, King Mongkut's Institute of Technology Ladkrabang (KMITL) is gratefully acknowledged. The authors also thank the Applied Analytical Chemistry Research Unit, Department of Chemistry, Faculty of Science, KMITL for instrumental support.

## Appendix A. Supplementary data

Supplementary data to this article can be found online at https://doi.org/10.1016/j.talanta.2019.120675.

## References


[1] D.B. Barr, L.C. Wilder, S.P. Caudill, A.J. Gonzalez, L.L. Needham, J.L. Pirkle, Urinary creatinine concentrations in the U.S. population: implications for urinary biologic monitoring measurements, Environ. Health Perspect. 113 (2) (2005) 192–200.

[2] T. Arndt, Urine-creatinine concentration as a marker of urine dilution: reflections using a cohort of 45,000 samples, Forensic Sci. Int. 186 (2009) 48–51.

[3] M. Jaffé, Ueber den Niederschlag, welchen Pikrinsäure in normalem Harn erzeugt und über eine neue Reaction des Kreatinins, Z. Physiol. Chem. 10 (1886) 391–400.

[4] J. Ogawa, W. Nirdnoy, M. Tabata, H. Yamada, S. Shimizu, A new enzymatic method for the measurement of creatinine involving a novel ATP-dependent enzyme, *N*-Methylhydantoin amidohydrolase, Biosci. Biotechnol. Biochem. 59 (12) (1995) 2292–2294.

[5] E. Liotta, R. Gottardo, L. Bonizzato, J.P. Pascali, A. Bertaso, F. Tagliaro, Rapid and direct determination of creatinine in urine using capillary zone electrophoresis, Clin. Chim. Acta 409 (2009) 52–55.

[6] Y.G. Zuo, C.J. Wang, J.P. Zhou, A. Sachdeva, V.C. Ruelos, Simultaneous determination of creatinine and uric acid in human urine by high-performance liquid chromatography, Anal. Sci. 24 (2008) 1589–1592.

[7] E.M.K. Leung, W. Chan, A novel reversed-phase HPLC method for the determination of urinary creatinine by pre-column derivatization with ethyl chloroformate: comparative studies with the standard *Jaffé* and isotope-dilution mass spectrometric assays, Anal. Bioanal. Chem. 406 (2014) 1807–1812.

[8] R.T. Ambrose, D.F. Ketchum, J.W. Smith, Creatinine determined by “high-performance” liquid chromatography, Clin. Chem. 29 (1983) 256–259.

[9] T. Sakai, H. Ohta, N. Ohno, Routine assay of creatinine in newborn baby urine by spectrophotometric flow-injection analysis, Anal. Chim. Acta 308 (1995) 446–450.

[10] K. Ponhong, N. Teshima, K. Grudpan, J. Vichapong, S. Motomizu, T. Sakai, Successive determination of urinary bilirubin and creatinine employing simultaneous injection effective mixing flow analysis, Talanta 133 (2015) 71–76.

[11] J. Sitanurak, P. Inpota, T. Mantim, N. Ratanawimarnwong, P. Wilairat, D. Nacapricha, Simultaneous determination of iodide and creatinine in human urine by flow analysis with an on-line sample treatment column, Analyst 140 (2015) 295–302.

[12] N. Choengchan, T. Mantim, P. Inpota, D. Nacapricha, P. Wilairat, P. Jittangprasert, W. Waiyawat, S. Fucharoen, P. Sirankpracha, N.P. Morales, Tandem measurements of iron and creatinine by cross injection analysis with application to urine from thalassemic patients, Talanta 133 (2015) 52–58.

[13] L. Gervais, N. de Rooji, E. Delamaeche, Microfluidic chips for point-of-care immunodiagnostics, Adv. Mater. 23 (2011) H151–H176.

[14] A.W. Martinez, S.T. Phillips, M.J. Butte, G.M. Whitesides, Patterned paper as a platform for inexpensive, low-volume, portable bioassays, Angew. Chem. Int. Ed. 46 (2007) 1318–1320.

[15] W.K.T. Coltro, D.P. de Jesus, J.A.F. da Silva, C.L. do Lago, E. Carrilho, Toner and paper-based fabrication techniques for microfluidic applications, Electrophoresis 31 (2010) 2487–2498.

[16] S. Byrnes, G. Thiessen, E. Fu, Progress in the development of paper-based diagnostics for low-resource point-of-care settings, Bioanalysis 5 (22) (2013) 2821–2836.

[17] E.W. Nery, L.T. Kubota, Sensing approaches on paper-based devices: a review, Anal. Bioanal. Chem. 405 (2013) 7573–7595.

[18] M. Santhiago, E.W. Nery, G.P. Santos, L.T. Kubota, Microfluidic paper-based devices for bioanalytical applications, Bioanalysis 6 (2014) 89–106.

[19] M. Ishii, P. Preechakasedkit, K. Yamada, O. Chailapakul, K. Suzuki, D. Citterio, Wax-assisted one-step enzyme-linked immunosorbent assay on lateral flow test devices, Anal. Sci. 34 (1) (2018) 51–56.

[20] K. Talalk, J. Noiphung, T. Songjaroen, O. Chailapakul, W. Laiwattanapaisal, A facile low-cost enzymatic paper-based assay for the determination of urine creatinine, Talanta 144 (2015) 915–921.

[21] J. Sittiwong, F. Unob, Paper-based platform for urinary creatinine detection, Anal. Sci. 32 (2016) 639–643.

[22] S. Sununta, P. Rattanarat, O. Chailapakul, N. Praphairaksit, Microfluidic paper-based analytical devices for determination of creatinine in urine samples, Anal. Sci. 34 (2018) 109–113.

[23] E.L. Rossini, M.I. Milani, E. Carriho, L. Pezza, H.R. Pezza, Simultaneous determination of renal function biomarkers in urine using a validated paper-based microfluidic analytical device, Anal. Chim. Acta 997 (2018) 16–23.

[24] S. Boobphahom, N. Ruecha, N. Rodthongkum, O. Chailapakul, V.T. Remcho, A copper oxide-ionic liquid/reduced graphene oxide composite sensor enabled by digital dispensing: non-enzymatic paper-based microfluidic determination of creatinine in human blood serum, Anal. Chim. Acta 1083 (2019) 110–118.

[25] C.A. Chaplan, H.T. Mitchell, A.W. Martinez, Paper-based standard addition assays, Anal. Methods. 6 (2014) 1296–1300.

[26] S.L.R. Ellison, M. Thompson, Standard additions: myth and reality, Analyst 133 (2008) 992–997.

[27] P. Kóscielniak, Nonlinear calibration by the standard addition method, Chemometr. Intell. Lab. Syst. 47 (1999) 275–287.

[28] F.A. Kappi, G.Z. Tsogas, D.C. Christodouleas, D.L. Giokas, Calibrant-loaded paper-based analytical devices for standard addition quantitative assays, Sens. Actuators B Chem. 253 (2017) 860–867.

[29] V.F. Curto, N. Lopez-Ruiz, L.F. Capitan-Vallvey, A.J. Palma, F. Benito-Lopez, D. Diamond, Fast prototyping of paper-based microfluidic devices by contact stamping using indelible ink, RSC Adv. 3 (2013) 18811–18816.

[30] P. de Tarso Garcia, T.M.G. Cardoso, C.D. Garcia, E. Carrilho, W.K.T. Coltro, A handheld stamping process to fabricate microfluidic paper-based analytical devices with chemically modified surface for clinical assays, RSC Adv. 4 (2014) 37637–37644.

[31] K.L. Dornelas, N. Dossi, E. Piccin, A simple method for patterning poly (dimethylsiloxane) barriers in paper using contact-printing with low-cost rubber stamps, Anal. Chim. Acta 858 (2015) 82–90.

[32] N. Lopez-Ruiz, V.F. Curto, M.M. Erenas, F. Benito-Lopez, D. Diamond, A.J. Palma, L.F. Capitan-Vallvey, Smartphone-based simultaneous pH and nitrite colorimetric determination for paper microfluidic devices, Anal. Chem. 86 (2014) 9554–9562.

[33] T.M.G. Gardoso, P.T. Garcia, W.K.T. Coltro, Colorimetric determination of nitrite in clinical, food and environmental samples using microfluidic devices stamped in paper platforms, Anal. Methods. 7 (2015) 7311–7317.

[34] H. Fu, J. Yang, L. Guo, J. Nie, Q. Yin, L. Zhang, Y. Zhang, Using the rubik’s cube to directly produce paper analytical devices for quantitative point-of-care aptamer-based assays, Biosens. Bioelectron. 96 (2017) 194–200.

[35] C. Duangdeewong, J. Sitanurak, P. Wilairat, D. Nacapricha, S. Teerasong, Microfluidic paper-based analytical device for convenient use in measurement of iodate in table salt and irrigation water, Microchem. J. 152 (2020) 104447.

[36] A. Mathaweesansurn, N. Maneerat, N. Choengchan, A mobile phone-based analyzer for quantitative determination of urinary albumin using self-calibration approach, Sens. Actuators B Chem. 242 (2017) 476–483.

[37] W. Wang, W.Y. Wu, W. Wang, J.J. Zhu, Tree-shaped paper strip for semi-quantitative colorimetric detection of protein with self-calibration, J. Chromatogr., A 1217 (2010) 3896–3899.

[38] W.J. Zhu, D.Q. Feng, M. Chen, Z.D. Chen, R. Zhu, H.L. Fang, W. Wang, Bienzyme colorimetric detection of glucose with self-calibration based on tree-shaped paper strip, Sens. Actuators B Chem. 190 (2014) 414–418.

[39] R.D. Deegan, O. Bakajin, T.F. Dupont, G. Huber, S.R. Nagel, T.A. Witten, Capillary flow as the cause of ring stains from dried liquid drops, Nature 389 (1997) 827–829.

[40] J.N. Miller, J.C. Miller, Statistics and Chemometrics for Analytical Chemistry, fourth ed., Pearson Education, 1993.

[41] J.D. Cook, Y.H. Caplan, C.P. LoDico, D.M. Bush, The characterization of human urine for specimen validity determination in workplace drug testing: a review, J. Anal. Toxicol. 24 (2000) 579–588.